

mosGraphGPT: a foundation model for multi-omic signaling graphs using generative AI

Heming Zhang^{1*}, Di Huang^{1*}, Emily Chen^{1,4,5}, Dekang Cao^{1,2}, Tim Xu^{1,2}, Ben Dizdar^{1,2}, Guangfu Li⁶, Yixin Chen², Philip Payne¹, Michael Province³, Fuhai Li^{1,4#}

¹Institute for Informatics, Data Science and Biostatistics (I2DB), Washington University School of Medicine, ²Department of Computer Science and Engineering, ³Division of Statistical Genomics, Department of Genetics, ⁴Department of Pediatrics, Washington University School of Medicine, Washington University in St. Louis, St. Louis, MO, USA. ⁵School of Arts and Sciences, University of Rochester, Rochester, NY, 14627, USA. ⁶Department of Surgery, School of Medicine, University of Connecticut, CT, 06032, USA. *Co-first authors. #Correspondence: Fuhai.Li@wustl.edu

Abstract - Generative pretrained models represent a significant advancement in natural language processing and computer vision, which can generate coherent and contextually relevant content based on the pre-training on large general datasets and fine-tune for specific tasks. Building foundation models using large scale omic data is promising to decode and understand the complex signaling language patterns within cells. Different from existing foundation models of omic data, we build a foundation model, *mosGraphGPT*, for multi-omic signaling (mos) graphs, in which the multi-omic data was integrated and interpreted using a multi-level signaling graph. The model was pretrained using multi-omic data of cancers in The Cancer Genome Atlas (TCGA), and fine-tuned for multi-omic data of Alzheimer's Disease (AD). The experimental evaluation results showed that the model can not only improve the disease classification accuracy, but also is interpretable by uncovering disease targets and signaling interactions. And the model code are uploaded via GitHub with link: <https://github.com/mosGraph/mosGraphGPT>

1. Introduction

Generative pretrained models have significantly advanced fields such as natural language processing and computer vision¹. These models are initially trained on extensive datasets and later fine-tuned for specific tasks, allowing them to produce coherent and contextually relevant content². In bioinformatics, the need for foundational models arises due to the complexity and volume of biological data³. Traditional models, like SVM or Autoencoders, often struggle with the variability in gene expression and the diverse conditions of cell types⁴. Foundation models overcome these challenges by learning generalized representations from large-scale datasets, capturing complex gene-gene and gene-cell interactions that simpler models cannot⁵. Additionally, foundation models benefit from extensive pretraining on massive datasets, efficiently extracting key features and outperforming traditional models that typically cannot generalize across different contexts without requiring extensively labeled datasets for specific tasks⁶.

Advancements in sequencing technologies have led to the generation of multi-omic data^{7,8}, which is essential for understanding the genetic diversity and complex signaling pathways at various levels within diseases, including cancer and Alzheimer's Disease (AD). The multi-omic datasets of cancer and AD are publicly available. However, the integrative multi-omic data analysis remains an open problem to identify the essential (sparse a few) signaling targets and signaling pathways from thousands of targets densely interacting with each other, interpreting the molecular mechanisms and novel therapeutic targets. AD is commonly defined using criteria such as the CERAD (Consortium to Establish a Registry for Alzheimer's Disease) score⁹, which evaluates the density of neurotic plaques to classify the severity of the disease. Many reports of omics data and analyses of AD have been published¹⁰⁻²⁵. However, the pathogenesis of AD remains unclear and there is a lack of effective prevention and curable treatment medications.

Compared to single-omic data analysis, integrating multi-omic datasets offers a comprehensive perspective on intricate and multi-layered biological processes. This integration enhances statistical power, enabling the identification of molecular mechanisms that involve crucial molecular targets and signaling pathways²⁶. Multi-omics data integration can improve the prediction and understanding of these conditions by revealing the genetic, transcriptomic, proteomic, and metabolomic alterations associated with disease progression and severity²⁷.

Proteins within cells function as part of systematic networks and modules, regulating complex biological processes and dysfunctional signaling pathways in diseases such as cancer²⁸. Several signaling pathways, such as those documented in KEGG²⁹, WikiPathways^{30,31}, and protein-protein interaction (PPI) databases like BioGRID^{32,33} and STRING^{34,35}, are publicly accessible. Graph neural network (GNN)-based models can effectively represent the flow and interactions within these signaling networks. The latent state of individual proteins is influenced by their multi-omics data features and the interacting proteins (neighbors) within the signaling network. Importantly, attention mechanisms can be employed to identify crucial targets and subsequent signaling pathways. Several models have been developed to integrate multi-omics data for a deeper understanding of complex diseases such as AD and Non-AD. Among them, M3NetFlow¹⁴ is a sophisticated model designed to incorporate multi-omics data into a graph-based framework. M3NetFlow leverages multi-hop information within each subgraph and employs global bi-directional message propagation to facilitate communication between genes and proteins. This approach enhances the inference process, allowing for a more nuanced understanding of the underlying biological processes³⁶. Another noteworthy model is mosGraphGen (multi-omics signaling graph generator)¹², which generates multi-omics signaling graphs for individual samples. This tool maps multi-omics data onto a biologically meaningful multi-level signaling network, enabling integrative and interpretable multi-omics data analysis using GNN models. By constructing these detailed signaling graphs, mosGraphGen provides

valuable insights into the multi-layered interactions within the biological systems of individual samples.

Building upon the strengths of these models, we propose a novel approach that further enhances the integration and analysis of multi-omics data. The graph foundation model aims to address the limitations of existing models by incorporating advanced generative pre-trained models and graph neural networks. By leveraging the extensive pretraining capabilities of foundation models, our approach can capture complex gene-gene and gene-cell interactions with higher accuracy and contextual relevance. In this study, we pre-trained the model using TCGA cancer multi-omic data³⁷, and fine-tuned the model using multi-omic data of AD to identify the key targets and signaling pathways of AD.

2. Methodology and Materials

2.1 Datasets

Multi-omics datasets of Alzheimer's Disease. The multi-omics data can be obtained from publicly available datasets, UCSC Xena and ROSMAP datasets (see **Tables 1-2**). After downloading the multi-omics data (including epigenomics, genomics, transcriptomics, proteomics, etc.) from these sources, the datasets will be converted into 2-dimensional data frames. These data frames will have columns for sample IDs, sample names, etc., and rows for probes, gene symbols, gene IDs, etc. To integrate multi-omics data with clinical data, identical samples across the datasets must be identified. Similarly, the process must involve converting rows (probes, gene symbols, gene IDs, etc.) into an identical standard: gene-level data by either aggregating the same measurements for each gene or eliminating duplicates due to gene synonyms. Genes are then aligned according to a reference genome, ensuring that the final annotation for each gene in the multi-omics data is accurate. Finally, standardizing gene counts across multi-omics datasets and addressing missing values by imputing with zeros or negative one values where necessary. After aligning all the columns to

standard sample IDs and all the rows to standard gene IDs and unifying identical number of samples and genes, the data were prepared for integration into Graph Neural Network (GNN) models. The epigenomics, genomics, transcriptomics, and proteomics data will be utilized as features of protein nodes within the GNN models.

KEGG regulatory network. Genes for constructing the knowledge graph were selected by intersecting multi-omics datasets with gene regulatory networks from the KEGG database, which comprises 2121 genes, 19751 protein-protein interactions and 26114 edges for UCSC Xena dataset; 2146 genes, 19867 protein-protein interactions and 26305 edges. After this intersection, the resulting number of entities in constructed biomedical knowledge graph was 8484 and 8584 for UCSC Xena and ROSMAP respectively.

Table 1. UCSC Database resources

Database	Description	Link
UCSC Xena DNA methylation (450k)	DNA methylation dataset generated using the Illumina Infinium HumanMethylation450 BeadChip array.	https://xenabrowser.net/datapages/?dataset=jhu-usc.edu_PANCAN_HumanMethylation450.betaValue_whitelisted.tsv.synapse_download_5096262.xena&host=https%3A%2F%2Fpancanatlas.xenahubs.net&removeHub=https%3A%2F%2Fxena.treehouse.gi.ucsc.edu%3A443
protein expression - RPPA	Quantifying protein expression	https://xenabrowser.net/datapages/?dataset=TCGA-RPPA-pancan-clean.xena&host=https%3A%2F%2Fpancanatlas.xenahubs.net&removeHub=https%3A%2F%2Fxena.treehouse.gi.ucsc.edu%3A443
somatic mutation (SNP and INDEL) - Gene level non-silent mutation	The TCGA Unified Ensemble "MC3" gene-level mutation dataset identifies somatic mutations in various cancers,	https://xenabrowser.net/datapages/?dataset=mc3.v0.2.8.PUBLIC.nonsilentGene.xena&host=https%3A%2F%2

	marking non-silent mutations (1) that alter protein sequences and wild type (0) for no mutations.	Fpancanatlas.xenahubs.net&removeHub=https%3A%2F%2Fxcna.treehouse.gi.ucsc.edu%3A443
Gene expression RNAseq - TOIL RSEM fpkm	gene expression data derived from RNAseq, processed using the TOIL pipeline, with expression levels estimated using RSEM and normalized as FPKM values.	https://xenabrowser.net/datapages/?dataset=tcga_RSEM_gene_fpkm&host=https%3A%2F%2Ftoil.xenahubs.net&removeHub=https%3A%2F%2Fxcna.treehouse.gi.ucsc.edu%3A443
GEO GPL16304 Platform	Illumina HumanMethylation450 BeadChip [UBC enhanced annotation v1.0]	https://www.ncbi.nlm.nih.gov/geo/query/acc.cgi?acc=GPL16304
Curated clinical data	Contains patient clinical features, achieved from paper "An Integrated TCGA Pan-Cancer Clinical Data Resource (TCGA-CDR) to drive high quality survival outcome analytics".	https://xenabrowser.net/datapages/?dataset=Survival_SupplementalTable_S1_20171025_xena_sp&host=https%3A%2F%2Fpancanatlas.xenahubs.net&removeHub=https%3A%2F%2Fxcna.treehouse.gi.ucsc.edu%3A443
Immune subtype	Model based immune subtype	https://xenabrowser.net/datapages/?dataset=Subtype_Immune_Model_Based.txt&host=https%3A%2F%2Fpancanatlas.xenahubs.net&removeHub=https%3A%2F%2Fxcna.treehouse.gi.ucsc.edu%3A443
Molecular subtype	Phenotype data	https://xenabrowser.net/datapages/?dataset=TCGASubtype.20170308.tsv&host=https%3A%2F%2Fpancanatlas.xenahubs.net&removeHub=https%3A%2F%2Fxcna.treehouse.gi.ucsc.edu%3A443
sample type and primary disease	sample type and primary disease information combined from all individual TCGA cohorts	https://xenabrowser.net/datapages/?dataset=TCGA_phenotype_denseDataOnlyDownload.tsv&host=https%3A%2F%2Fpancanatlas.xenahubs.net&removeHub=https%3A%2F%2Fxcna.treehouse.gi.ucsc.edu%3A443

Table 2. ROSMAP Database resources

Database	Description	Link
ROSMAP_arrayMethylation_imputed	Methylation data was generated on prefrontal cortex samples collected from 708 individuals using the Illumina HumanMethylation450 BeadChip	https://www.synapse.org/#!Synapse:syn3168763
C2.median_polish_corrected_log2(Proteomics)	Data generated from isobaric TMT peptide labeling of ROSMAP brain tissues were submitted to the AD Knowledge Portal in two rounds. Round 1 (submitted in 2018) provides data from 400 individuals. Round 2 (submitted in 2022) provides data from an additional 210 individuals.	https://www.synapse.org/#!Synapse:syn21266454
ROSMAP_RNAseq_FPKM_gene	Samples were extracted using Qiagen's miRNeasy mini kit (cat. no. 217004) and the RNase free DNase Set (cat. no. 79254), and quantified by Nanodrop and quality was evaluated by Agilent Bioanalyzer.	https://www.synapse.org/#!Synapse:syn3505720
ROSMAP.CNV.Matrix(Mutation)	The TCGA Unified Ensemble "MC3" gene-level mutation dataset identifies somatic mutations in various cancers, marking non-silent mutations (1) that alter protein sequences and wild type (0) for no mutations.	https://www.synapse.org/#!Synapse:syn26263118
GEO GPL16304 Platform	Illumina HumanMethylation450 BeadChip [UBC enhanced annotation v1.0]	https://www.ncbi.nlm.nih.gov/geo/query/acc.cgi?acc=GPL16304
ROSMAP_clinical	Contains patient clinical features. A large amount of clinical and pathological data have been collected from individuals in the ROSMAP studies. The remainder of the clinical and pathological data may be accessed directly from the Rush Alzheimer's Disease Center.	https://www.synapse.org/#!Synapse:syn3191087

2.2 The mosGraphGPT model

Problem Formulation The overall architecture of mosGraphGPT model was demonstrated in **Figure 1**. Given the bulk-seq multi-omics datasets of $\mathcal{X}^{(Epi)}$ for

epigenomics, $\mathcal{X}^{(\text{Geno})}$ for genomics, $\mathcal{X}^{(\text{Tran})}$ for transcriptomics and $\mathcal{X}^{(\text{Prot})}$ for proteomics and clinical dataset $\mathcal{Y}^{(c)}$, the integration over biomedical knowledge graph was completed by mosGraphGen² with $\mathcal{G} = (V, E)$, which can be decomposed into subgraphs $\mathcal{G}_{\text{int}} = (V_{\text{int}}, E_{\text{int}})$, where $|V_{\text{int}}| = n_{\text{Epi}} + n_{\text{Geno}} + n_{\text{Tran}} + n_{\text{Prot}} = n = |V|$ and $\mathcal{G}_{\text{PPI}} = (V_{\text{PPI}}, E_{\text{PPI}})$, where $|V_{\text{PPI}}| = n_{\text{Prot}}$ and $\mathcal{G}_{\text{int}} = \mathcal{G} \setminus \mathcal{G}_{\text{PPI}}$. Correspondingly, adjacency matrix $A \in \mathbb{R}^{n \times n}$ for whole graph \mathcal{G} will be generated and adjacency matrix $A_{\text{int}} \in \mathbb{R}^{n \times n}$ for internal signaling flows from promoters to proteins via central dogma. What's more, protein-protein interactions will be represented by adjacency matrix $A_{\text{PPI}} \in \mathbb{R}^{n \times n}$ and $A = A_{\text{int}} + A_{\text{PPI}}$. Furthermore, patient multi-omics feature $\mathcal{X} = \{X^{(1)}, X^{(2)}, \dots, X^{(m)}, \dots, X^{(M)}\}$ will be generated, where $X^{(m)} \in \mathbb{R}^{n \times d}$, d equals the number of multi-omics data features and n equals the number of nodes. With above processed pretraining datasets, the encoder model, $f_{\text{pre}}(\cdot)$, will be pretrained by self-supervised learning by reconstructing edges and degree of nodes. Similarly, the input bulk-seq multi-omics datasets with clinical features can also be generated with $\mathcal{X}' = \{X'^{(1)}, X'^{(2)}, \dots, X'^{(k)}, \dots, X'^{(K)}\}$ and $\mathcal{Y}' = \{y'^{(1)}, y'^{(2)}, \dots, y'^{(k)}, \dots, y'^{(K)}\}$ ($X'^{(k)} \in \mathbb{R}^{n \times d}$, $y'^{(k)} \in \mathbb{R}^{C'}$ and C' is the number of patient types). Regarding the biomedical knowledge graph, internal signaling flows graph, protein-protein interactions graph, all of them share the same network structures with \mathcal{G} , \mathcal{G}_{int} , \mathcal{G}_{PPI} and adjacency matrices A , A_{int} , A_{PPI} . Hence, the similar graph structures were generated by \mathcal{G}' , $\mathcal{G}'_{\text{int}}$, $\mathcal{G}'_{\text{PPI}}$ and adjacency matrices A' , A'_{int} , A'_{PPI} . And our proposed model can be denoted as $f(\cdot)$ to predict the patient types with $\widehat{\mathcal{Y}} = f(\mathcal{X}', A')$.

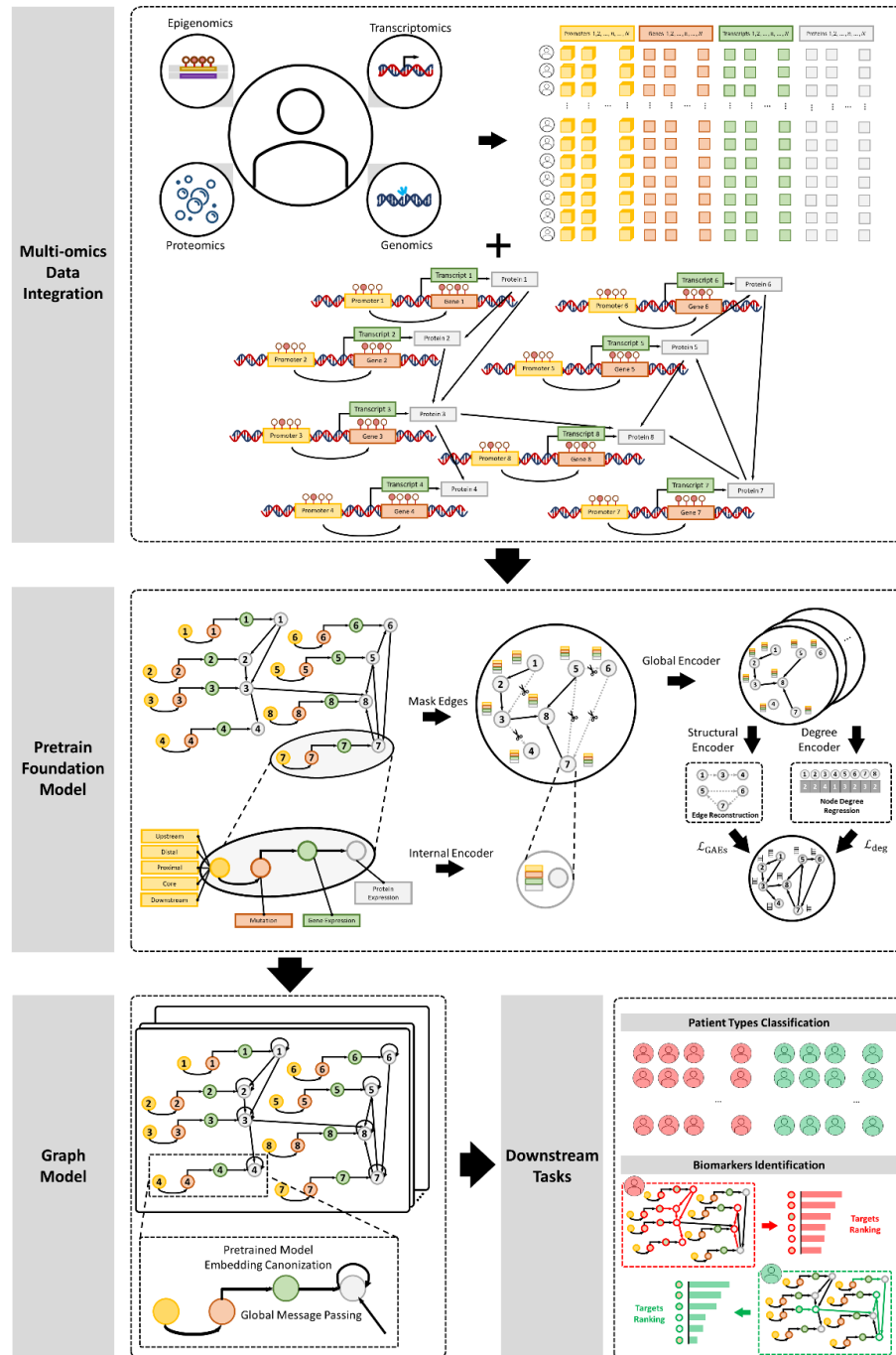


Figure 1. Architecture of *mosGraphGPT*.

Pretrain Foundation Model During the pretraining stage, the constructed biomedical knowledge graph A can be decomposed into 2 subgraph paths A_{int} and A_{ppi} , where message propagation will also be separated with 2 steps for internal signaling flows from promoters to proteins and protein signaling flows between protein-protein interactions. Since, it is the protein-protein interactions that the *mosGraphGPT* model

would like to reconstruct, earlier stage message passing was accomplished to propagate information to the protein nodes with:

$$H_{\text{int}}^{(m)} = \text{GNN}_{\text{int}}(X^{(m)}, A_{\text{int}}) \quad (1)$$

, where $H_{\text{int}}^{(m)} \in \mathbb{R}^{n \times d_{\text{int}}}$ is the node features which was diffused from epigenomics, genomics, transcriptomics and proteomics onto the ending protein nodes and GNN_{int} is the internal signaling flows encoder. Meanwhile, to mask the edges for pretrain model to reconstruct, the random masking function Γ will be generated following a specific distribution, e.g., Bernoulli distribution:

$$E_{\text{mask}} \sim \text{Bernoulli}(p) \quad (2)$$

, where $p < 1$ is the ratio of the masked edges for the protein-protein interactions graph \mathcal{G}_{PPI} . Hence, the masked protein-protein interactions graph will be denoted as $\mathcal{G}_{\text{mask}}$ and the unmasked or visual protein-protein interactions graph will be denoted as \mathcal{G}_{vis} , where $\mathcal{G}_{\text{PPI}} = \mathcal{G}_{\text{vis}} \cup \mathcal{G}_{\text{mask}}$. Correspondingly, the masked adjacency matrix A_{mask} and visual adjacency matrix A_{vis} will be generated by the masking function Γ . Afterwards, the global encoder will be used to generate the node embeddings by

$$H^{(m)} = \text{GNN}_{\text{global}}(H_{\text{int}}^{(m)}, A) \quad (3)$$

, where $H^{(m)} \in \mathbb{R}^{n \times d_{\text{global}}}$ and $\text{GNN}_{\text{global}}$ is the graph neural network message propagation for signaling flows in global paths. With the global node embeddings, structural decoder and degree decoder were built to learn the pretrain model. In details, the structural decoder u_{ω} with parameters ω will decode to probability of the edge connection between node p and q by

$$u_{\omega}(h_p^{(m)}, h_q^{(m)}) = \sigma\left(\text{MLP}\left(h_p^{(m)} \odot h_q^{(m)}\right)\right) \quad (4)$$

, where $h_p^{(m)}, h_q^{(m)} \in \mathbb{R}^{d_{\text{global}}}$ are global node embedding for node p and q for patient m ; MLP is the multilayer perceptron and \odot is the element-wise product. Moreover, the degree decoder v_{ϕ} was constructed by

$$v_{\phi}(h_p^{(m)}) = \text{MLP}\left(h_p^{(m)}\right) \quad (5)$$

, where ϕ is the parameter learnt from the degree decoder and the decoder aims to reconstruct the node degree with regression.

In sum, the pretrain model reconstruction loss, $\mathcal{L}^{(m)}$, will be calculated by edge reconstruction loss, which measures how well the model can rebuild the edge connect in the protein-protein interactions network and degree regression loss, which measures how closely the prediction of the node degree matches the degree of nodes in original graph \mathcal{G} with

$$\mathcal{L}^{(m)} = \mathcal{L}_{\text{GAEs}}^{(m)} + \mathcal{L}_{\text{deg}}^{(m)} \quad (6)$$

, where edge reconstruction loss, $\mathcal{L}_{\text{GAEs}}$, is self-supervised learning objective loss by optimizing the cross-entropy loss via

$$(\mathcal{L}^{(m)})^+ = \frac{1}{|E^+|} \sum_{(p,q) \in E^+} \log u_{\omega}(h_p^{(m)}, h_q^{(m)}) \quad (7)$$

$$(\mathcal{L}^{(m)})^- = \frac{1}{|E^-|} \sum_{(p,q) \in E^-} \log(1 - u_{\omega}(h_p^{(m)}, h_q^{(m)})) \quad (8)$$

$$\mathcal{L}_{\text{GAEs}}^{(m)} = -((\mathcal{L}^{(m)})^+ + (\mathcal{L}^{(m)})^-) \quad (9)$$

, where E^+ is a set of positive edges while E^- is a set of negative edges sampled from the protein-protein interaction graph \mathcal{G}_{PPI} and degree reconstruction loss will be calculated with mean squared error (MSE) between the original degree of nodes and the predicted ones

$$\mathcal{L}_{\text{deg}}^{(m)} = \frac{1}{|V|} \sum_{p \in V} \left\| v_{\phi}(h_p^{(m)}) - \text{deg}(p^{(m)}) \right\|_F^2 \quad (10)$$

, where $\text{deg}(\cdot)$ is the degree function which can generate the degree of node p for patient m over whole graph \mathcal{G} .

Graph Model Construction With the pretrained encoder function $f_{\text{pre}}: \mathbb{R}^d \rightarrow \mathbb{R}^{d_{\text{pre}}}$ composed of internal encoder and global encoder shown in formula (1) and (3), the input feature can generate embedding $H^{(k)} = f_{\text{pre}}(X^{(k)})$ which can be used as the graph canonization via residual process with

$$H'_{\text{mix}}{}^{(k)} = \text{CONCAT} \left[X'^{(k)}, H'^{(k)} \right] \quad (11)$$

, where $H'_{\text{mix}}{}^{(k)} \in \mathbb{R}^{d+d_{\text{pre}}}$ is the concatenated node features for patient k . To predict the patient k outcome, the global message propagation was conducted via

$$Z'^{(k)} = \text{GNN}_{\text{final}} \left(H'_{\text{mix}}{}^{(k)}, A' \right) \quad (12)$$

, where $Z'^{(k)} \in \mathbb{R}^{d_{\text{final}}}$ and transformer-based message passing network was leveraged here as the $\text{GNN}_{\text{final}}$. The cross-entropy (CE) function was used via

$$\mathcal{L}'^{(k)} = \text{CE} \left(y'^{(k)}, \text{MLP} \left(\text{AVG} \left[Z'^{(k)} \right] \right) \right) \quad (13)$$

, where mean aggregation pooling function AVG in PyTorch and linear transformation with MLP was leverage.

2.3 Downstream Tasks

Predict patient types Given the embedded features $Z'^{(k)}$ for patient k , the prediction of the patient type can be generated by

$$\widehat{y}'^{(k)} = \arg \max \left(\text{MLP} \left(\text{AVG} \left[Z'^{(k)} \right] \right) \right) \quad (14)$$

, where $\widehat{y}'^{(k)} \in \mathbb{R}$.

Biomarkers Identification via Attention Based on the attention extracted from transformer, the weighted adjacency matrix $A'_w{}^{(k)} \in \mathbb{R}^{n \times n}$ will be generated. Furthermore, the average weighted adjacency matrix of specific patient type c can be calculated by

$$[A'_w]^{(c)} = \frac{1}{|\mathcal{X}'^{(c)}|} \sum_{k \in \mathcal{X}'^{(c)}} A'_w{}^{(k)} \quad (15)$$

, where $\mathcal{X}'^{(c)}$ is the set of specific patient type c .

3. Results

3.1 mosGraphGPT model results

Experimental settings The UCSC xena multi-omics dataset was used as the pretrain model, which contains 3592 cancer patients with 2121 genes, 8484 node entities, 19751 protein-protein interactions and 26114 relations. Early stopping strategies was employed for self-supervised pretraining process. Afterwards, for training the whole model, ROSMAP was loaded with 128 samples with 2146 genes, 8584 node entities, 19867 protein-protein interactions and 26305 relations. Specifically, the 5 fold cross validation was used to train and test the proposed model, *mosGraphGPT*. To evaluate the model performance in terms of synergy score prediction for drug combinations, we conducted 5-fold cross validation. The *mosGraphGPT* model was implemented using PyTorch and PyTorch Geometric, with the Adam optimizer of setting weight decay as 1×10^{-20} and ϵ as 1×10^{-7} employed for training.

Model performance and comparison The average prediction accuracy was about **75.09%** the test data on ROSMAP AD dataset. The results indicated the feasibility of patient outcome prediction using a graph neural network with a small set of core signaling pathways genes. Moreover, the proposed model was compared with other graph neural networks (see **Table 3**), which included the GNN model with mean aggregation in transductive mode³⁸ (no sampling for neighborhood function) and Graph Attention network³⁹ (GAT), Graph Isomorphism Network (GIN)⁴⁰ and UniMP⁴¹.

Table 3. Model comparison with other GNN networks (AD vs. Non-AD)

Models	Fold 1	Fold 2	Fold 3	Fold 4	Fold 5	Avg \pm Std
GCN	56.00%	76.00%	72.00%	64.00%	64.29%	66.46% \pm 6.96%
GAT	68.00%	76.00%	68.00%	72.00%	53.57%	67.51% \pm 7.58%
GIN	52.00%	72.00%	64.00%	64.00%	71.43%	64.69% \pm 7.22%
UniMP	52.00%	72.00%	72.00%	76.00%	71.43%	68.69% \pm 8.50%
mosGraphGPT	68.00%	80.00%	76.00%	80.00%	71.43%	75.09% \pm 4.75%

3.2 Downstream tasks

To investigate the potential MoS, a core signaling subnetwork was generated based on the trained model. Specifically, the integrated signaling flow networks were obtained from the large signaling network based on the averaged trained directional weight matrices on the 5 splits of test datasets on ROSMAP-AD. With averaging the attention weight adjacency matrices $[A'_w]^{(ADi)}$ and $[A'_w]^{(Non-ADi)}$ ($i = 1, 2, \dots, 5$) on each fold, the weight adjacency matrices $[A'_w]^{(AD)}$ for AD samples and $[A'_w]^{(Non-AD)}$ for Non-AD samples are generated. Afterwards, the cell line specific gene degrees will be calculated based on following formula:

$$d_i^{(c)} = \left(\sum_{j=1}^n a_c^{(ij)} \right) \quad (16)$$

, where $a_c^{(ij)}$ is the element in the i -th row and j -th column of the matrices $[A'_w]^{(AD)}$ for AD samples ($c = AD$) and $[A'_w]^{(Non-AD)}$ for Non-AD patients ($c = Non - AD$), which measures the link strength between node i and node j . Hence, $d_i^{(c)}$ is the weighted degree for node i from specific sample type c .

Afterwards, the unimportant signaling flows in the attention-based matrix for certain type of patient will be filtered out by

$$W_F^{(c)} = F(W^{(c)}, \theta) \quad (8)$$

, where $F(\cdot)$ is the filtering mapping function by providing selection of each element in the matrix with

$$F(w, \theta) = \begin{cases} w, & \text{if } w > \theta \\ 0, & \text{if } w \leq \theta \end{cases} \quad (9)$$

, where $w \in \mathbb{R}$ is the element in the input matrix and $W_F^{(c)} \in \mathbb{R}^{n^{(prot)} \times n^{(prot)}}$ is the filtered matrix. Hence, the filtered node set for patient type c , $V_F^{(c)}$, will be generated by removing independent nodes and nodes in those small connected components with number of nodes lower than ϕ , resulting in $|V_F^{(c)}|$ nodes.

Subsequently, p-values for the gene features, such as methylations in promoter nodes, mutations and genes expression in gene nodes and proteins expression in protein nodes were calculated. The p-value calculation for these features was conducted by using the chi-squared test to check the differences between AD/non-AD samples or female/male of AD patients. This statistical method determined whether there were significant differences in the gene features between the samples of AD/non-AD or female/male from AD. By constructing contingency tables and performing the chi-squared test for each gene feature, p-values indicating the statistical significance of the observed differences were obtained. Ultimately, the top T gene features associated with AD or gender were selected based on these p-values.

After finalized important gene features ranked by p-values in top T , the network was pruned by iteratively removing the nodes which are only connected to one another unimportant node in a linear branch with node recursive algorithm (check details of this algorithm in **Appendix A** and **Figure S1**). This ensures that each remaining nodes is either linked to an important node or is part of a more complex interaction network, enhancing the purity and reliability of the gene interaction data.

Subsequently, nodes degree were calculated to identify hub node (node degree larger than 2). The set of middle nodes for certain path t which connects two hub nodes u and v can be denoted as $P_{u \rightarrow v}^{(t)} = \{n_1, n_2, \dots, n_r, \dots, n_R\}^{(t)}$, where $\lambda + 1$ is the length of path. Hence, the average edge weight on the path $P_{u \rightarrow v}^{(t)}$ can be generated by

$$O_{u \rightarrow v}^{(t)} = \frac{1}{\lambda} \sum_{r=1}^{\lambda-1} W_{n_r, n_{r+1}}^{(c)} \quad (10)$$

, where $W_{n_r, n_{r+1}}^{(c)}$ is the edge weight from node n_r to node n_{r+1} . For all of the paths detected between the hub node u and hub node v , the nodes on the top β paths will be kept. Additionally, p-value middle nodes, which are crucial due to their statistical

significance, will be retained along with middle nodes that are adjacent to these p-value nodes. (check **Appendix Section A.2** for details).

Uncovering AD associated targets and signaling pathways Setting the edge threshold θ as 0.15 and filtering out small components with nodes fewer than 25 ($\phi=25$), the core signaling network flows for AD and non-AD samples were generated. The AD core signaling network included 335 potential important protein nodes, and the non-AD network contained 408 potential important protein nodes. To further discover the top 100 important node entities in the whole network, p-value was leveraged to measure the importance of the nodes in this core signaling network. Visualization of the core signaling networks were also accomplished with the pruning algorithm (check **Appendix A**) to mark the important nodes in the network (shown in **Figures 2-4**). Through the polished algorithm, the AD network was refined to 256 protein nodes and the non-AD network to 267 protein nodes. This significantly reduced the impact of irrelevant nodes on the core signaling networks visualization, providing a clearer depiction of protein-protein interactions.

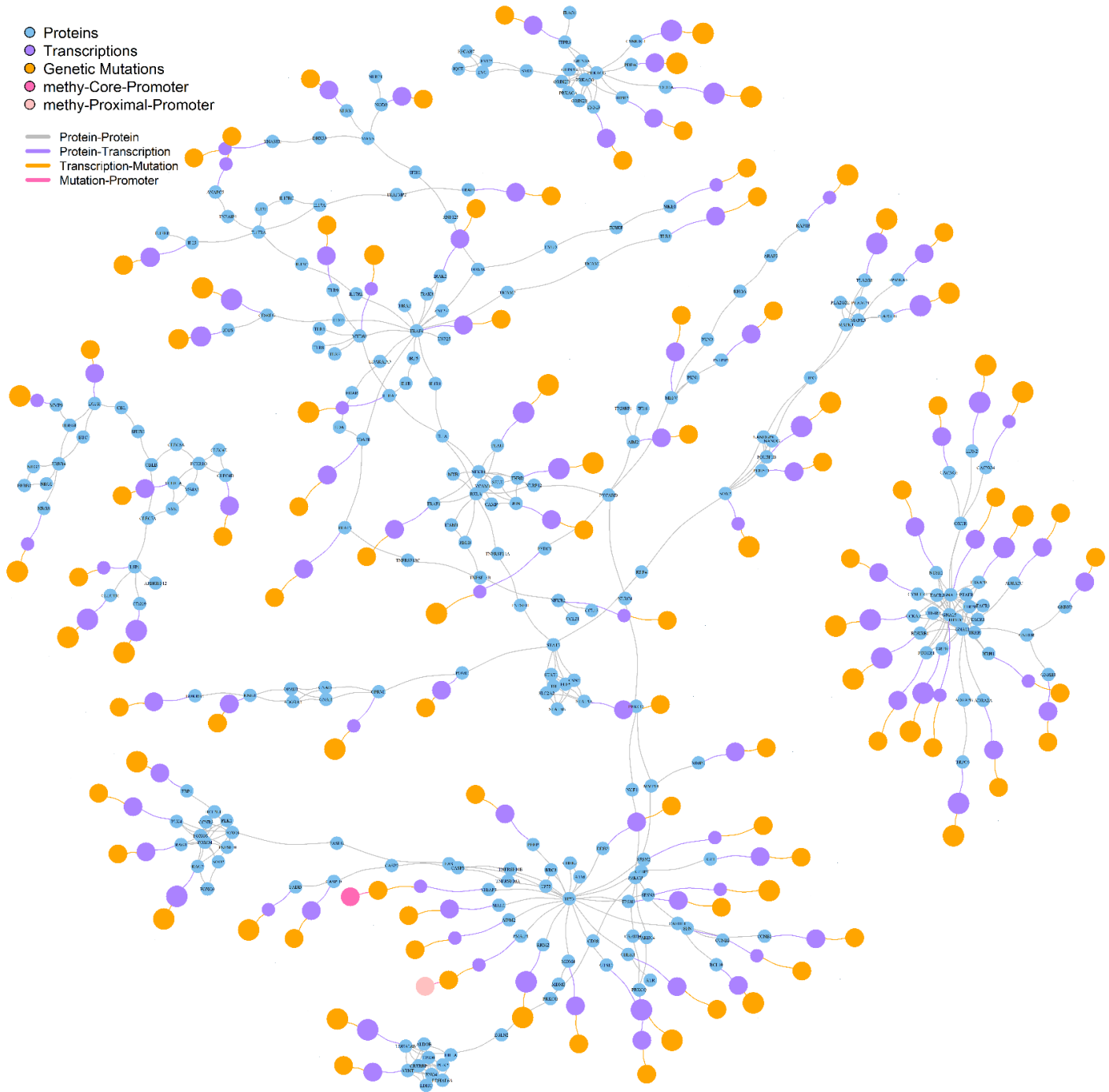


Figure 2. Important signaling network flows for AD patients with top 100 gene features ranked by p-values

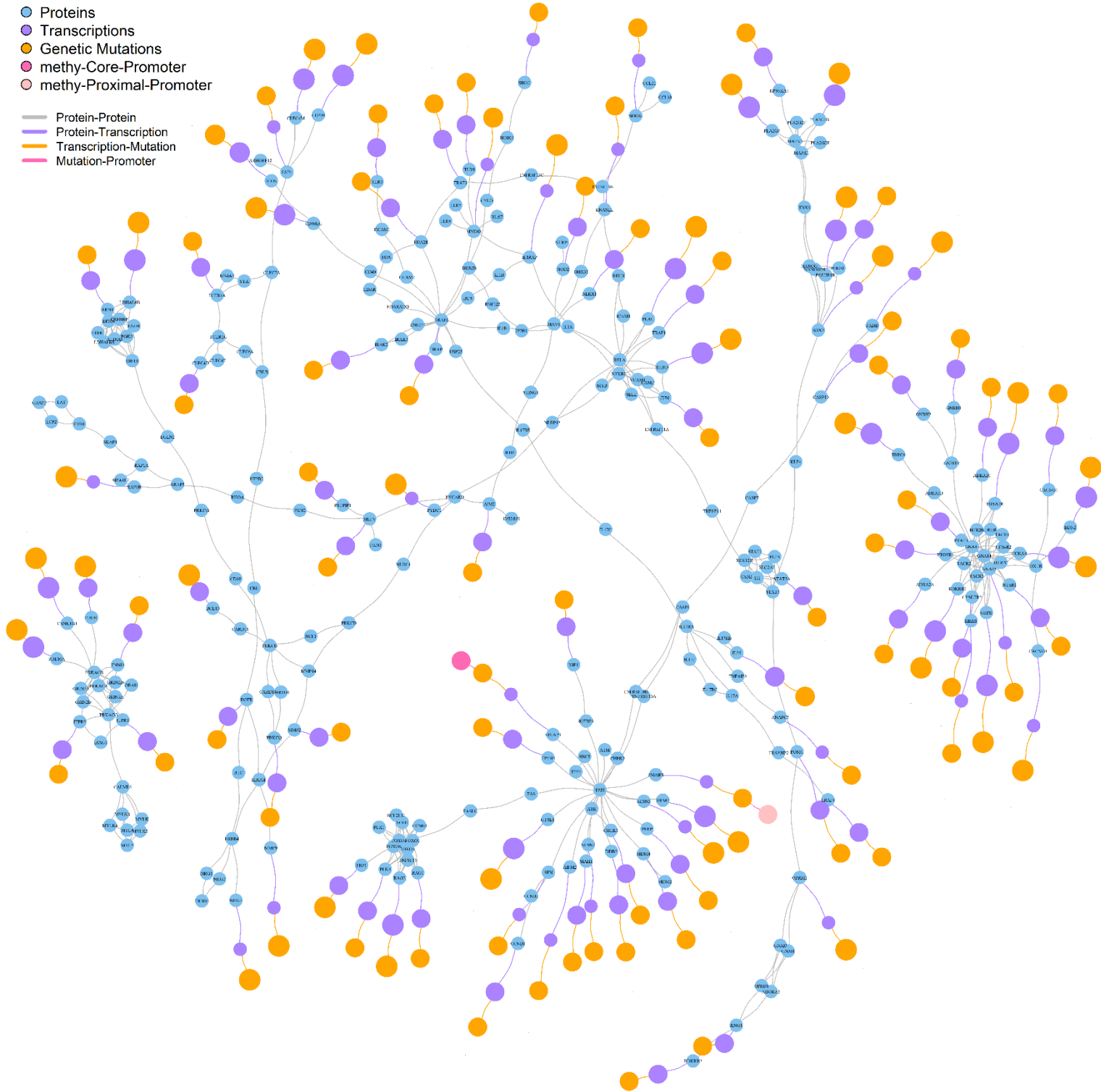


Figure 3. Important signaling network flows for non-AD patients with top 100 gene features ranked by p-values

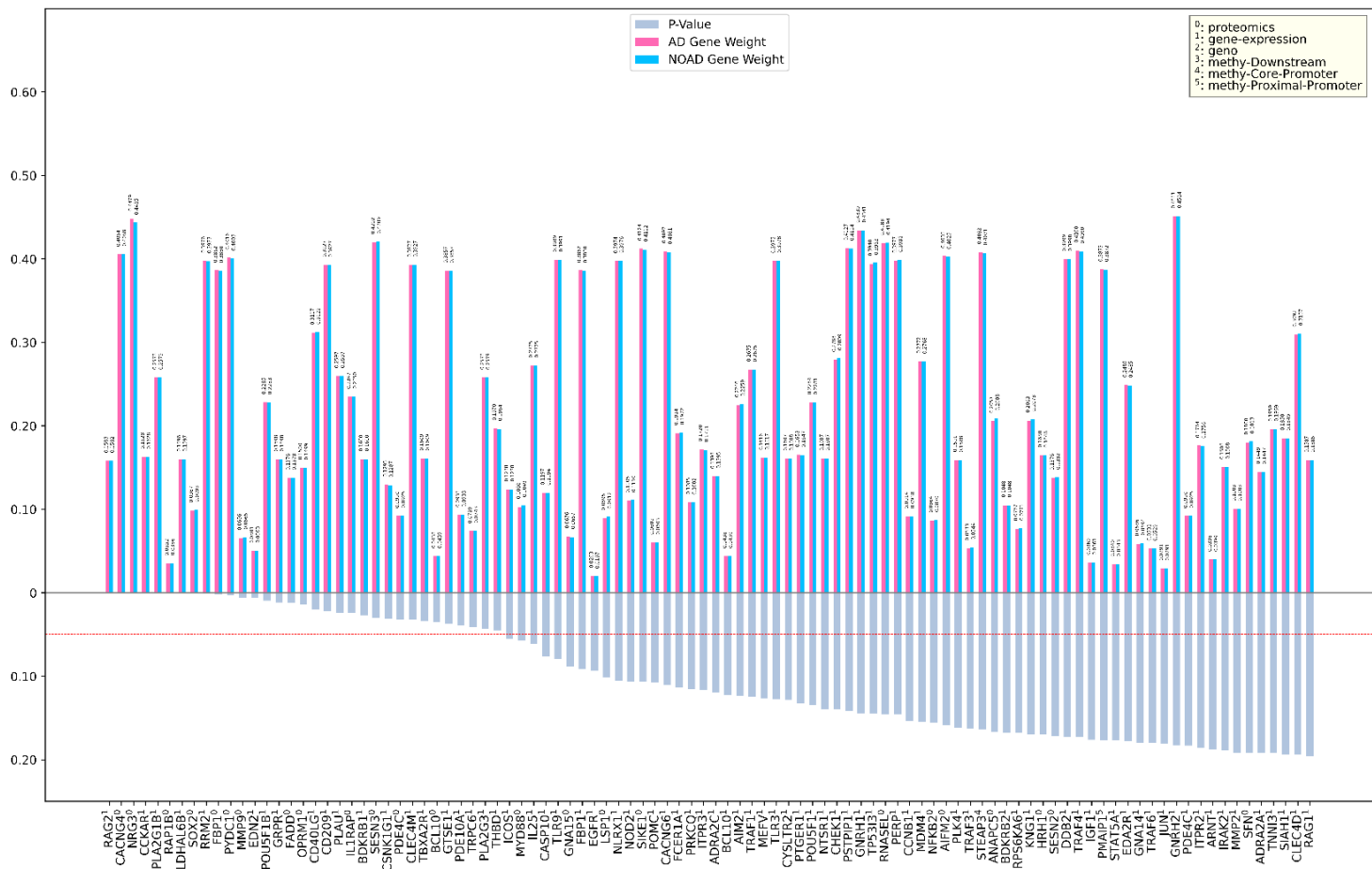


Figure 4. Top 100 important gene features for AD samples ranked by p-value

3.3 Validation on identified biomarkers

Based on the top 100 gene features, which include promoters, mutations, transcriptions, and proteins, selected for Alzheimer's disease (AD) samples through the use of p-values, a comprehensive validation process has been undertaken. This selection was made to identify the most statistically significant gene features relevant to AD, thereby enabling a focused analysis of the underlying biological mechanisms.

The subsequent validation involved conducting a pathway enrichment analysis, which is a critical step in understanding the functional implications of these gene features.

This analysis helps to identify biological pathways that are significantly enriched in the dataset, providing insights into the molecular processes and pathways that may be disrupted in AD. The results of this pathway enrichment analysis are presented in

Figures 5-6 and detailed in **Table 4**. These findings are essential for corroborating the

initial selection of gene features and for highlighting potential targets for further investigation. The integration of these results into the broader context of AD research underscores the importance of pathway enrichment analysis in validating genetic and molecular data, thus contributing to a more nuanced understanding of the disease's pathogenesis and potential therapeutic avenues.

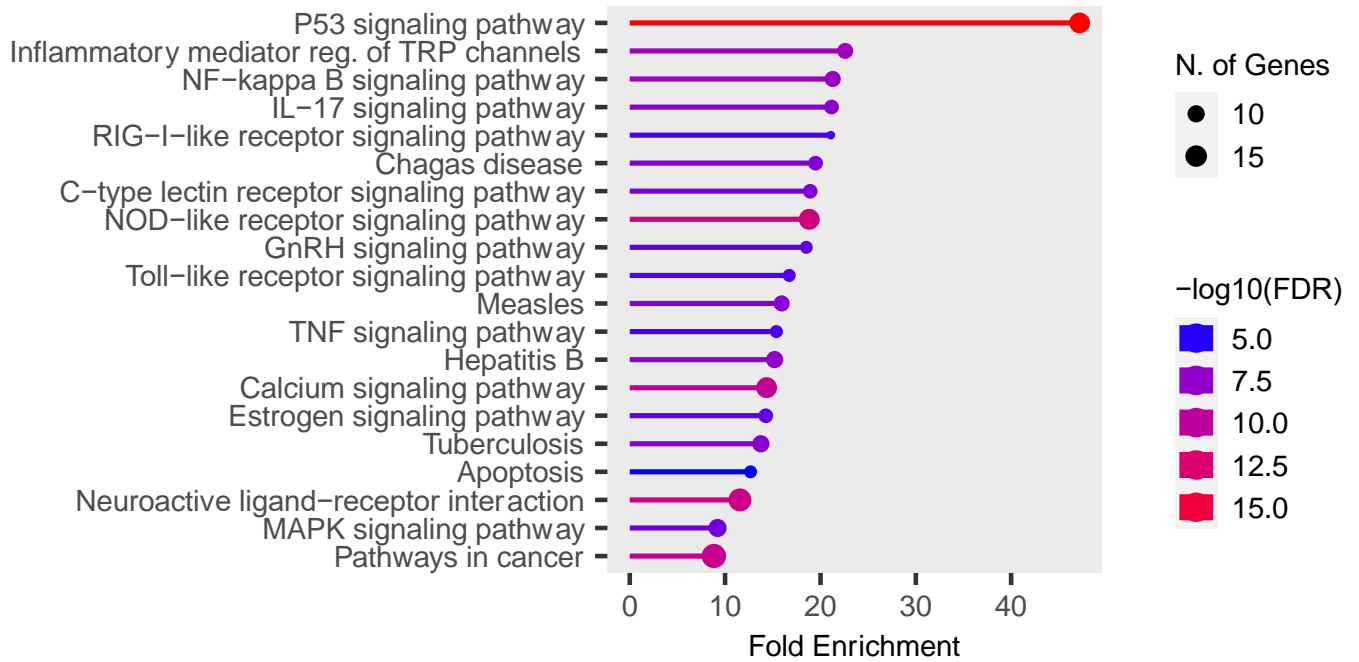


Figure 5. Top 20 pathways lollipop plot

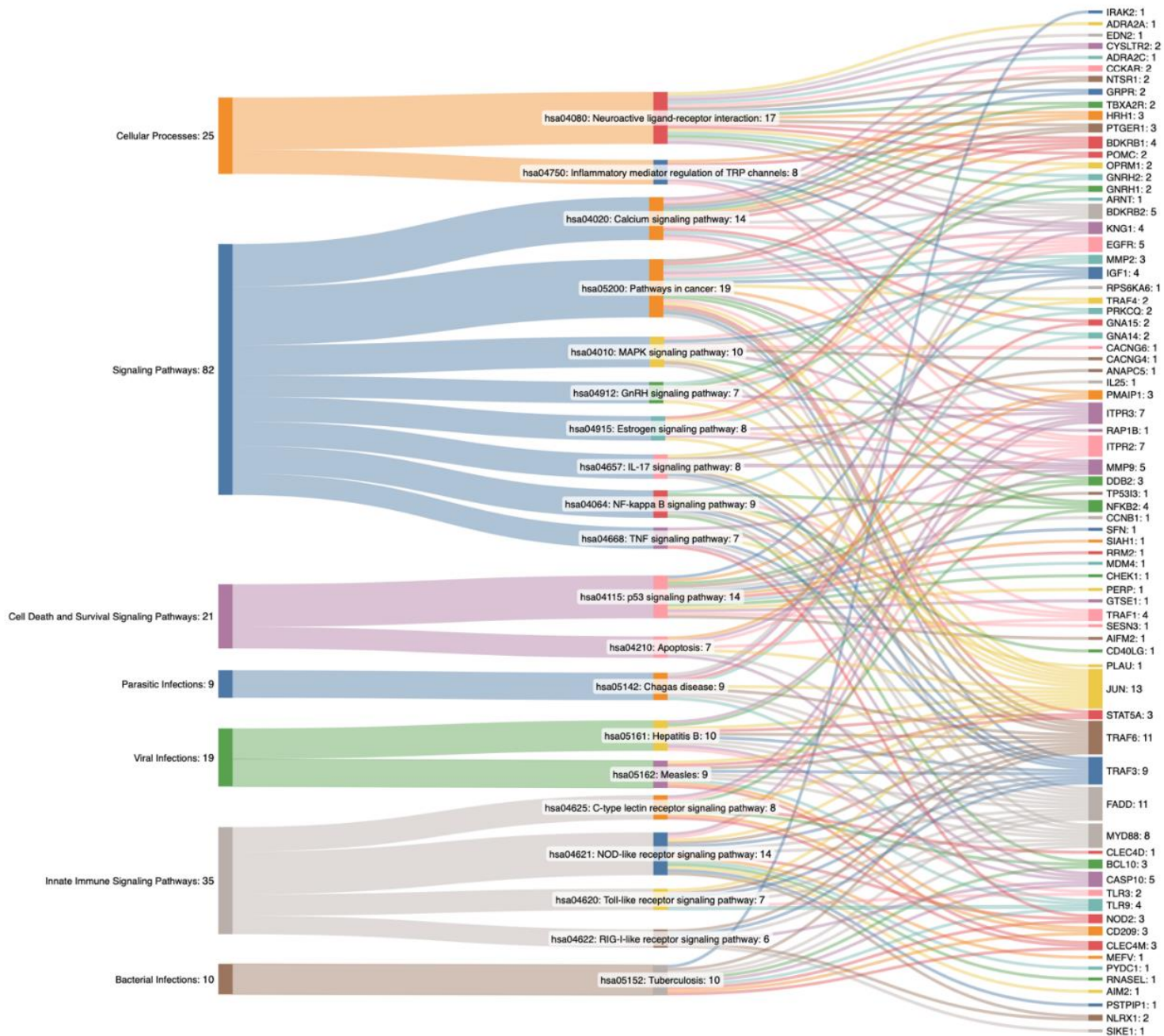


Figure 6. Top 20 pathways Sankey chart

Table 4. Pathway enrichment analysis for top 20 gene features ranked by p-values

Type	Pathway	Number of Genes	Genes	P-Value	FDR
Signaling Pathways	hsa05200: Pathways in cancer	19	BDKRB1,MMP2,DDB2,TRAF4,KNG1,EGFR,PTGER1,FADD,IGF1	6.1E-12	4.1E-10

			,PMAIP1,STAT5A,ARNT,NFKB2, JUN,MMP9,TRAF1,TRAF6,BDK RB2,TRAF3		
Cellular Processes	hsa04080: Neuroactive ligand-receptor interaction	17	BDKRB1,GNRH2,KNG1,GNRH1, ADRA2A,CYSLTR2,PTGER1,CC KAR,NTSR1,EDN2,GRPR,HRH1 ,POMC,ADRA2C,TBXA2R,OPR M1,BDKRB2	5.42E-13	6.07E-11
Cell Death and Survival Signalig Pathways	hsa04115: p53 signaling pathway	14	TP53I3,CCNB1,DDB2,IGF1,PMA IP1,SFN,SIAH1,RRM2,MDM4,C HEK1,PERP,GTSE1,SESN3,AIF M2	3.49E-18	1.17E-15
Innate Immune Signalig Pathways	hsa04621: NOD-like receptor signaling pathway	14	MEFV,NOD2,FADD,PYDC1,RNA SEL,AIM2,JUN,ITPR3,ITPR2,NL RX1,MYD88,TRAF6,PSTPIP1,T RAF3	2.52E-13	4.23E-11
Signaling Pathways	hsa04020: Calcium signaling pathway	14	BDKRB1,GNA15,EGFR,CYSLTR 2,PTGER1,CCKAR,NTSR1,ITPR 3,GNA14,GRPR,ITPR2,HRH1,TB XA2R,BDKRB2	9.45E-13	7.94E-11
Viral Infections	hsa05161: Hepatitis B	10	DDB2,CASP10,TLR3,FADD,STA T5A,JUN,MMP9,MYD88,TRAF6, TRAF3	7.38E-09	3.1E-07
Bacterial Infections	hsa05152: Tuberculosis	10	IRAK2,CASP10,NOD2,FADD,CD 209,CLEC4M,TLR9,BCL10,MYD 88,TRAF6	1.21E-08	4.53E-07

Signaling Pathways	hsa04010: MAPK signaling pathway	10	RAP1B,CACNG6,CACNG4,RPS6KA6,EGFR,IGF1,NFKB2,JUN,MYD88,TRAF6	1.47E-06	2.9E-05
Parasitic Infections	hsa05142: Chagas disease	9	GNA15,KNG1,FADD,TLR9,JUN,GNA14,MYD88,TRAF6,BDKRB2	2.13E-09	1.19E-07
Signaling Pathways	hsa04064: NF-kappa B signaling pathway	9	PRKCQ,NFKB2,BCL10,CD40LG,PLAU,TRAF1,MYD88,TRAF6,TRAF3	2.51E-09	1.2E-07
Viral Infections	hsa05162: Measles	9	FADD,CD209,CLEC4M,STAT5A,TLR9,JUN,MYD88,TRAF6,TRAF3	3.22E-08	9.02E-07
Signaling Pathways	hsa04657: IL-17 signaling pathway	8	ANAPC5,TRAF4,FADD,IL25,JUN,MMP9,TRAF6,TRAF3	2.41E-08	8.09E-07
Cellular Processes	hsa04750: Inflammatory mediator regulation of TRP channels	8	BDKRB1,PRKCQ,KNG1,IGF1,ITPR3,ITPR2,HRH1,BDKRB2	2.81E-08	8.6E-07
Innate Immune Signaling Pathways	hsa04625: C-type lectin receptor signaling pathway	8	CLEC4D,CD209,CLEC4M,NFKB2,BCL10,JUN,ITPR3,ITPR2	5.1E-08	1.32E-06
Signaling Pathways	hsa04915: Estrogen signaling pathway	8	MMP2,EGFR,JUN,MMP9,ITPR3,ITPR2,POMC,OPRM1	3.5E-07	8.39E-06
Signaling Pathways	hsa04912: GnRH signaling pathway	7	MMP2,GNRH2,EGFR,GNRH1,JUN,ITPR3,ITPR2	3.57E-07	8.39E-06
Innate Immune Signaling Pathways	hsa04620: Toll-like receptor signaling pathway	7	TLR3,FADD,TLR9,JUN,MYD88,TRAF6,TRAF3	7.97E-07	1.67E-05

Signaling Pathways	hsa04668: TNF signaling pathway	7	CASP10,NOD2,FADD,JUN,MMP9,TRAF1,TRAF3	1.54E-06	2.9E-05
Cell Death and Survival Signaling Pathways	hsa04210: Apoptosis	7	CASP10,FADD,PMAIP1,JUN,TRAF1,ITPR3,ITPR2	4.33E-06	7.28E-05

Cell Death and Survival Signaling As a crucial transcription factor, p53 regulates DNA repair, cell cycle control, apoptosis, and oxidative stress response. In AD, p53 function is notably disrupted, leading to increased DNA damage and impaired repair mechanisms. Elevated phosphorylated p53 levels and altered oligomerization states in AD patients' temporal lobes indicate compromised DNA damage response and repair capabilities⁴². p53 also forms oligomers and fibrils that interact with tau oligomers, potentially seeding further p53 aggregation and mislocalization outside the nucleus, impairing its nuclear functions⁴³. This aggregation and tau interaction may contribute to lethal cell cycle re-entry and abnormal cell death in AD. Additionally, p53 signaling intersects with other dysregulated pathways in AD, such as WNT and NFkB, particularly in inhibitory neurons, where decreased p53 activity and altered transcription factor activity are observed⁴⁴. The complexity of p53's role in AD is heightened by its regulation through post-translational modifications, affecting its conformation and function, and potentially influencing amyloid and tau pathways⁴⁵. Oxidative stress in AD patients exacerbates p53 dysfunction, as indicated by increased protein carbonylation and impaired cGAS-STING-interferon signaling, crucial for immune-stimulated DNA repair⁴².

Apoptosis is a programmed cell death mechanism essential for maintaining cellular homeostasis and regulating cell turnover, but its dysregulation can lead to neurodegenerative disorders, including AD^{46,47}. In AD, several pathological features such as A β plaques, hyperphosphorylated tau tangles, inflammation, mitochondrial

dysfunction, and oxidative stress trigger an abnormal apoptotic cascade in critical brain regions like the cerebral cortex and hippocampus⁴⁶. This cascade involves various molecular pathways, including PI3K/AKT, JNK, MAPK, and mTOR signaling, which ultimately result in neuronal death and correlate with the severity of dementia⁴⁶. Additionally, apoptosis interacts with necroptosis, another form of programmed cell death, which is also activated in AD brains and contributes to neuroinflammation and neuronal death⁴⁸⁻⁵⁰. The interplay between apoptosis and necroptosis exacerbates the neurodegenerative process, as necroptosis can be triggered by factors such as hyperglycemia and reactive oxygen species, which are prevalent in AD. Therapeutic strategies targeting apoptotic pathways, such as caspases and other apoptotic regulators, have been explored to mitigate neuronal loss and slow disease progression^{46,47}.

Signaling Pathways NF- κ B signaling is central to neuroinflammation and oxidative stress, exacerbating neurodegeneration by interacting with reactive microglia, astrocytes, and various molecular factors, while also influencing amyloid plaque clearance and neuronal survival⁵¹. Dysregulated calcium signaling disrupts neuronal function and survival by causing mitochondrial failure, oxidative stress, and chronic neuroinflammation, leading to NFTs and A β plaques⁵². The ER-mitochondria membrane contact site is particularly critical for calcium homeostasis, and its disruption further exacerbates AD pathology⁵³. Estrogen signaling, particularly in women, plays a multifaceted role in AD, with estrogen deficiency post-menopause promoting amyloid precursor protein processing into senile plaques and increasing tau phosphorylation⁵⁴. Estrogen also affects glucose metabolism and WNT signaling, contributing to neuropathology. The interaction between estrogen and APOE genotype modulates AD risk, with estrogen receptors' reduced activity accelerating disease progression⁵⁵.

GnRH, along with luteinizing hormone (LH) and activins, possesses neuronal receptors that are distributed throughout the limbic system, which is crucial for cognitive functions and is notably affected in AD⁵⁶. Dysregulation of the HPG axis

during menopause and andropause leads to elevated levels of GnRH and LH, while sex steroid signaling decreases, potentially promoting neurodegenerative changes⁵⁶. Elevated LH levels, which are a consequence of this dysregulation, have been implicated in the amyloidogenic processing of APP^{56,57}. Furthermore, LH is known to cross the blood-brain barrier and its receptors are highly concentrated in the hippocampus, a region particularly vulnerable to AD⁵⁶. Pharmacological interventions that suppress LH release, such as leuprolide acetate, have shown promise in reducing A β deposition and improving cognitive performance in animal models of AD, suggesting a potential therapeutic avenue^{56,57}. Epidemiological data also support this connection, as reduced neurodegenerative disease incidence has been observed among prostate cancer patients treated with GnRH agonists, which lower LH levels⁵⁶.

Dysregulation of MAPK signaling, particularly through the ERK/MAPK1 pathway, has been implicated in the development of AD pathogenesis⁵⁸. Specifically, phosphorylated ERK (p-ERK) has been identified as a critical regulator of pro-inflammatory activation of microglia, which are immune cells in the brain that contribute to neuroinflammation in AD^{59,60}. This pro-inflammatory state is further exacerbated by the JAK/STAT signaling pathway, which is activated by overactive microglia and astrocytes, leading to a chronic neuroinflammatory environment that is characteristic of AD. Additionally, the PI3K-Akt pathway, which interacts with MAPK signaling, is involved in regulating cell survival and metabolic functions, and its dysregulation is linked to A β and NFTs⁶¹. The complex interplay between these pathways is evident as the PKR/P38/RIPK1 signaling axis, part of the stress-activated MAPK pathway, is highly activated in AD brains, leading to A β accumulation, tau phosphorylation, and cognitive decline⁶². Experimental models have shown that modulating miRNAs that regulate MAPK signaling can improve cognitive deficits, highlighting the therapeutic potential of targeting this pathway⁶¹.

In AD, TNF signaling has been implicated in promoting necroptosis. This is evidenced by increased expression of necroptosis-related proteins such as phosphorylated

RIPK3 and MLKL in the AD brain, particularly in CA1 pyramidal neurons, which correlates inversely with neuron density⁶³. Additionally, TNF exposure in human iPSC-derived neurons increases necroptotic cell death, which can be mitigated by inhibitors targeting RIPK1, RIPK3, and MLKL, suggesting potential therapeutic intervention points⁶³. Furthermore, TNF-mediated neuroinflammation is exacerbated by the interaction of misfolded proteins with pattern recognition receptors on astroglia and microglia, leading to the release of inflammatory mediators that contribute to disease progression⁶⁴. Genome-wide analyses have identified several genes associated with sporadic AD that control inflammatory responses and glial clearance of misfolded proteins, highlighting the critical role of immune processes in AD pathogenesis⁶⁴. Interestingly, patients with rheumatoid arthritis and other systemic inflammatory diseases treated with TNF- α blocking agents show a reduced probability of developing dementia, suggesting that TNF- α inhibition could be a viable strategy for preventing AD and preserving cognitive function⁶⁵.

Studies have shown that IL-17A levels are elevated in the brains of AD patients and animal models, suggesting its involvement in disease progression^{66,67}. When IL-17A is overexpressed, worsening of cognitive functions is observed⁶⁷. IL-17A also exacerbates neuroinflammation by facilitating the infiltration of immune cells such as CD8+ T lymphocytes and myeloid cells into the brain, which in turn accelerates the production of pro-inflammatory chemokines like CXCL1 and CXCL9/10 by glial cells⁶⁷. This inflammatory milieu promotes A β accumulation and synaptic dysfunction, leading to cognitive deficits. Furthermore, IL-17A has been shown to induce neural damage directly when administered to primary hippocampal neurons, and its inhibition via neutralizing antibodies can ameliorate A β -induced neurotoxicity and cognitive decline by downregulating the TRAF6/NF- κ B pathway⁶⁶. Additionally, the depletion of gut bacteria, which reduces IL-17A-expressing T cells, has been found to lower cerebral A β levels and inhibit inflammatory activation in the brain, highlighting the gut-brain axis's role in AD pathophysiology⁶⁸.

Innate Immune Signaling Pathways The NOD-like receptor signaling pathway, particularly the NLRP3 inflammasome, promotes the release of proinflammatory cytokines such as IL-1 β and IL-18, exacerbating neuroinflammation and contributing to AD progression⁶⁹. This pathway is further activated by dysregulated ions like K⁺ and Ca²⁺, prevalent in AD, which heightens the inflammatory response⁶⁹. TLR signaling, notably through TLR3 and TLR4, influences A β dynamics and mediates neuroinflammation. TLR4 activation by A β in microglia triggers proinflammatory cytokine production, leading to amyloid-dependent neuronal death⁷⁰. Similarly, dysregulated TLR pathways activate NF- κ B and MAPK pathways, resulting in further inflammation and apoptosis⁷¹. The RLR pathway, although primarily known for antiviral responses, may exacerbate AD by promoting chronic inflammation through cytokine production. Lastly, T cells, particularly CD8⁺ T cells, infiltrate the brain and cerebrospinal fluid of AD patients, displaying increased expression of inflammatory pathways and significant clonal expansion⁷². Studies have demonstrated that T cells, especially cytotoxic T cells, are markedly increased in areas with tau pathology, correlating with neuronal loss and dynamically transforming from activated to exhausted states, which indicates their involvement in neurodegeneration⁷³. Furthermore, the depletion of T cells has been shown to block tau-mediated neurodegeneration, suggesting that T cell activity directly contributes to disease progression⁷³.

C-type lectin receptors (CLRs), such as CLEC-2, are found on the surface of platelets and are involved in the regulation of intestinal barrier function through their interaction with zonulin, a key modulator of intestinal permeability. Elevated levels of CLEC-2 and zonulin have been observed in patients with mild cognitive impairment and AD, suggesting a link between gut permeability and AD pathology. These elevated levels are also associated with reduced cognitive function as measured by the Mini-Mental State Examination score⁷⁴. Additionally, CLRs are expressed by myeloid cells and recognize pathogen-associated molecular patterns and damage-associated molecular patterns, initiating immune responses that can contribute to inflammation, a known risk

factor for AD⁷⁵. Specifically, the scavenger receptor with C-type lectin (SRCL) has been implicated in the clearance of A β . SRCL is upregulated in astrocytes and vascular cells in AD patients and mouse models, suggesting its role in binding and clearing A β , thereby potentially mitigating AD progression⁷⁶. Furthermore, the Dectin-1 cluster of CLRs, which includes receptors like CLEC-2, is involved in various pathophysiological processes, including inflammation and immune regulation, both of which are critical in the context of AD.

Cellular Processes Neuroactive ligand-receptor interactions maintain brain homeostasis and regulate neurotransmitter systems, inflammatory responses, and neuroprotective mechanisms. In AD, disruptions in ligand-receptor networks, particularly those involving inflammatory pathways, are significant. For instance, microglial receptors interact with danger-associated molecular patterns to clear neurotoxic substances like A β and hyperphosphorylated tau^{77,78}. Impairments in these interactions reduce the clearance of these toxic proteins, exacerbating disease progression. Chemokines and their receptors, part of neuroactive ligand-receptor interactions, have a dual role in AD: promoting neuroprotection and synaptic plasticity under normal conditions but leading to chronic inflammation when overexpressed, further contributing to A β aggregation and tau hyperphosphorylation⁷⁹. Neurotransmitter receptors, such as cholinergic, glutamatergic, and serotonergic receptors, are also modulated in response to AD pathology, affecting cognitive functions and contributing to symptoms like memory loss and cognitive decline⁸⁰. Multi-target-directed ligands that modulate these neurotransmitter systems show promise in providing symptomatic relief and potentially modifying disease progression by targeting multiple pathways involved in AD, including neuroinflammation and oxidative stress⁸¹. Therefore, understanding and targeting neuroactive ligand-receptor interactions offer significant potential for developing therapeutic strategies to combat AD.

TRP channels, such as TRPV1 and TRPA1, are implicated in the regulation of inflammatory processes in the brain. TRPV1, a non-selective cation channel, is involved in neuroinflammation and has been shown to influence microglial function. Activation of TRPV1 can rescue microglial dysfunction, restore metabolic impairments, and enhance immune responses, thereby reducing amyloid pathology and memory deficits in AD models^{82,83}. On the other hand, TRPA1 channels, predominantly expressed in astrocytes, are activated by A β and mediate Ca²⁺ influx, which in turn triggers the production of pro-inflammatory cytokines and activation of transcription factors such as NF- κ B and NFAT. Inhibition of TRPA1 channels reduces A β -induced inflammation and behavioral dysfunction, highlighting their role in AD pathogenesis⁸⁴. Additionally, TRPC channels, particularly TRPC6, have been implicated in AD development, suggesting that TRP channels broadly contribute to the disease through their involvement in calcium homeostasis and glial cell activation⁸⁵. The regulation of these channels by inflammatory mediators underscores their potential as therapeutic targets. Pharmacological modulation of TRP channels, such as using TRPV1 agonists, has shown promise in alleviating AD symptoms by reducing neuroinflammation and improving cellular functions^{82,83}.

Bacterial Infections Studies show tuberculosis (TB) patients have a higher risk of AD, potentially due to TB-induced chronic inflammation, which is a known AD risk factor⁸⁶. Treatments for TB, like the BCG vaccine and rifampicin, show potential in modulating immune responses and reducing neuroinflammation, which could slow AD progression⁸⁷. Again, maintaining gut and managing bacterial infections promptly, might mitigate risks for AD.

Viral Infections Measles virus (MeV) has been implicated in neurodegenerative processes, as seen in subacute sclerosing panencephalitis, where persistent infection leads to neurofibrillary tangle formation, similar to AD⁸⁸. This suggests that viral infections can contribute to neurodegenerative changes. The immune response to MeV, characterized by prolonged virus clearance and immunosuppression, may create

a chronic inflammatory environment conducive to neurodegeneration⁸⁹. Liver function markers, such as elevated AST to ALT ratios, are associated with AD diagnosis and cognitive dysfunction, suggesting metabolic disturbances linked to liver function influence AD pathophysiology⁹⁰.

Hepatitis B virus (HBV), though less directly linked to AD, has been explored for its potential therapeutic avenues. Innovative research using HBV core protein to develop a vaccine targeting truncated tau proteins showed promising results in reducing tau pathology and cognitive deficits in a mouse model⁹¹.

Parasitic Infections Chagas disease is primarily known for its impact on cardiac and gastrointestinal systems, but its potential role in the pathogenesis of AD can be inferred through its immunological and inflammatory mechanisms. The chronic infection with *T. cruzi* leads to a persistent inflammatory response and structural derangement in cardiac tissues, which is a hallmark of Chagas heart disease⁹². This inflammatory process is driven by the host's immune response to the parasite, involving altered immunoregulatory mechanisms and pathogen persistence. Similarly, AD is characterized by neuroinflammation, where the accumulation of misfolded proteins activates an innate immune response, releasing inflammatory mediators that exacerbate the disease⁹³. The cGAS–STING signaling pathway, which triggers type-I interferon-mediated neuroinflammation, is a critical component in AD pathogenesis⁹³. Given that Chagas disease involves significant immune activation and inflammation, it is plausible that *T. cruzi* infection could influence neuroinflammatory pathways similar to those seen in AD. Additionally, the vascular pathogenesis of Chagas disease, involving functional changes in vasoactive peptides like endothelin-1 and kinins, could further contribute to neurovascular dysfunction, a known factor in AD progression⁹⁴. Thus, while direct evidence linking Chagas disease to Alzheimer's disease is limited, the shared mechanisms of chronic inflammation and immune dysregulation provide a basis for further investigation into their potential connection.

4. Discussion and conclusion

This study introduces mosGraphGPT, a generative pre-trained model designed for the integration and interpretation of multi-omics data. The primary aim was to enhance the understanding of Alzheimer's disease (AD) pathogenesis by identifying significant signaling pathways and potential biomarkers through advanced graph neural networks (GNNs). The novel approach leverages extensive pre-training capabilities to capture complex gene-gene and gene-cell interactions with high accuracy and contextual relevance.

The integration of multi-omics data is crucial for understanding the intricate and multi-layered biological processes underlying complex diseases such as AD. Traditional models often struggle with the variability in gene expression and the diverse conditions of cell types. In contrast, foundation models like mosGraphGPT learn generalized representations from large-scale datasets, capturing complex interactions that simpler models cannot. This study utilized multi-omics datasets from UCSC Xena, encompassing epigenomics, genomics, transcriptomics, and proteomics data. The comprehensive dataset included 3592 cancer patients, 2121 genes, 8484 node entities, 19751 protein-protein interactions, and 26114 relations.

The experimental evaluation demonstrated that mosGraphGPT significantly improved disease classification accuracy and interpretability by uncovering disease targets and signaling interactions. The model achieved an average prediction accuracy of 75.09% on the ROSMAP AD dataset, outperforming other graph neural networks such as GCN, GAT, GIN, and UniMP. The results indicate the feasibility of patient outcome prediction using a GNN with a small set of core signaling pathways genes. The model's ability to identify biomarkers and key signaling pathways was validated through attention mechanisms and statistical analyses. The integration of multi-omics data allowed for the identification of molecular mechanisms involving crucial molecular targets and signaling pathways. Notably, pathways such as the p53 signaling pathway, NF-kappa

B signaling, and MAPK signaling were highlighted as significant in the context of AD. These findings are consistent with existing literature, underscoring the importance of these pathways in neurodegenerative diseases.

The findings from this study have significant implications for the field of bioinformatics and precision medicine. The ability of mosGraphGPT to integrate and interpret multi-omics data at a granular level provides a robust framework for understanding complex diseases. Future research could expand this model to other diseases and incorporate additional omics data to further refine the understanding of disease mechanisms and therapeutic targets. Additionally, the application of such models in clinical settings could enhance the precision of diagnostic and therapeutic strategies, paving the way for more personalized medicine approaches.

In conclusion, mosGraphGPT represents a significant advancement in the integration and interpretation of multi-omics data. By leveraging the extensive capabilities of generative pre-trained models and graph neural networks, this study has provided valuable insights into the molecular mechanisms of Alzheimer's disease. The findings highlight the potential of such models to revolutionize the field of bioinformatics and precision medicine, offering a powerful tool for the study of complex diseases.

Acknowledgement

This study was partially supported by NIA R56AG065352, 1R21AG078799-01A1, 1RM1NS132962-01, 1R01LM013902-01A1.

References

1. Mirra S, Heyman A, McKeel D, et al. *The Consortium to Establish a Registry for Alzheimer's Disease (CERAD). Part 11. Standardization of the Neuropathologic Assessment of Alzheimer's Disease*. Vol 41.; 2024. <https://www.neurology.org>

2. Hasin Y, Seldin M, Lusic A. Multi-omics approaches to disease. *Genome Biol.* 2017;18(1). doi:10.1186/s13059-017-1215-1
3. Karczewski KJ, Snyder MP. Integrative omics for health and disease. *Nat Rev Genet.* 2018;19(5):299-310. doi:10.1038/nrg.2018.4
4. Huang S, Chaudhary K, Garmire LX. More is better: Recent progress in multi-omics data integration methods. *Front Genet.* 2017;8(JUN). doi:10.3389/fgene.2017.00084
5. Moffitt RA, Marayati R, Flate EL, et al. Virtual microdissection identifies distinct tumor- and stroma-specific subtypes of pancreatic ductal adenocarcinoma. *Nat Genet.* 2015;47(10):1168-1178. doi:10.1038/ng.3398
6. Devlin J, Chang MW, Lee K, Toutanova K. BERT: Pre-training of Deep Bidirectional Transformers for Language Understanding. Published online October 10, 2018. <http://arxiv.org/abs/1810.04805>
7. Brown TB, Mann B, Ryder N, et al. Language Models are Few-Shot Learners. Published online May 28, 2020. <http://arxiv.org/abs/2005.14165>
8. Min S, Lee B, Yoon S. Deep learning in bioinformatics. *Brief Bioinform.* 2017;18(5):851-869. doi:10.1093/bib/bbw068
9. Noble WS. *What Is a Support Vector Machine?* Vol 24.; 2006. <http://www.nature.com/naturebiotechnology>
10. Zou J, Huss M, Abid A, Mohammadi P, Torkamani A, Telenti A. A primer on deep learning in genomics. *Nat Genet.* 2019;51(1):12-18. doi:10.1038/s41588-018-0295-5
11. Lecun Y, Bengio Y, Hinton G. Deep learning. *Nature.* 2015;521(7553):436-444. doi:10.1038/nature14539
12. Zhang H, Cao D, Chen Z, et al. mosGraphGen: a novel tool to generate multi-omic signaling graphs to facilitate integrative and interpretable graph AI model development. doi:10.1101/2024.05.15.594360
13. Zhang H, Chen Y, Payne P, Li F. Mining signaling flow to interpret mechanisms of synergy of drug combinations using deep graph neural networks. doi:10.1101/2021.03.25.437003

14. Zhang H, Goedegebuure SP, Ding L, et al. M3NetFlow: a novel multi-scale multi-hop multi-omics graph AI model for omics data integration and interpretation. doi:10.1101/2023.06.15.545130
15. De Jager PL, Ma Y, McCabe C, et al. A multi-omic atlas of the human frontal cortex for aging and Alzheimer's disease research. *Sci Data*. 2018;5(1):1-13.
16. Bennett DA, Buchman AS, Boyle PA, Barnes LL, Wilson RS, Schneider JA. Religious Orders Study and Rush Memory and Aging Project. *Journal of Alzheimer's Disease*. 2018;64(s1):S161-S189. doi:10.3233/JAD-179939
17. Allen M, Carrasquillo MM, Funk C, et al. Human whole genome genotype and transcriptome data for Alzheimer's and other neurodegenerative diseases. *Sci Data*. 2016;3. doi:10.1038/sdata.2016.89
18. Wang M, Roussos P, McKenzie A, et al. Integrative network analysis of nineteen brain regions identifies molecular signatures and networks underlying selective regional vulnerability to Alzheimer's disease. *Genome Med*. 2016;8(1). doi:10.1186/s13073-016-0355-3
19. Li F, Eteleeb AM, Buchser W, et al. Weakly activated core neuroinflammation pathways were identified as a central signaling mechanism contributing to the chronic neurodegeneration in Alzheimer's disease. *Front Aging Neurosci*. 2022;14. doi:10.3389/fnagi.2022.935279
20. Li F, Oh I, Kumar S, et al. Loss of estrogen unleashing neuro-inflammation increases the risk of Alzheimer's disease in women. doi:10.1101/2022.09.19.508592
21. Feng J, Province M, Li G, Payne PRO, Chen Y, Li F. PathFinder: a novel graph transformer model to infer multi-cell intra- and inter-cellular signaling pathways and communications. doi:10.1101/2024.01.13.575534
22. Dong Z, Zhao Q, Payne PRO, et al. Highly Accurate Disease Diagnosis and Highly Reproducible Biomarker Identification with PathFormer. Published online February 11, 2024. doi:10.21203/rs.3.rs-3576068/v1
23. Wan YW, Al-Ouran R, Mangleburg CG, et al. Meta-Analysis of the Alzheimer's Disease Human Brain Transcriptome and Functional Dissection in Mouse Models. *Cell Rep*. 2020;32(2). doi:10.1016/j.celrep.2020.107908
24. Raj T, Li YI, Wong G, et al. Integrative transcriptome analyses of the aging brain implicate altered splicing in Alzheimer's disease susceptibility. *Nat Genet*. 2018;50(11):1584-1592. doi:10.1038/s41588-018-0238-1

25. McKenzie AT, Moyon S, Wang M, et al. Multiscale network modeling of oligodendrocytes reveals molecular components of myelin dysregulation in Alzheimer's disease. *Mol Neurodegener.* 2017;12(1). doi:10.1186/s13024-017-0219-3
26. Wang M, Li A, Sekiya M, et al. Transformative Network Modeling of Multi-omics Data Reveals Detailed Circuits, Key Regulators, and Potential Therapeutics for Alzheimer's Disease. *Neuron.* 2021;109(2):257-272.e14. doi:10.1016/j.neuron.2020.11.002
27. Neff RA, Wang M, Vatansever S, et al. *Molecular Subtyping of Alzheimer's Disease Using RNA Sequencing Data Reveals Novel Mechanisms and Targets.* Vol 7.; 2021. <https://www.science.org>
28. Vidal M, Cusick ME, Barabási AL. Interactome networks and human disease. *Cell.* 2011;144(6):986-998. doi:10.1016/j.cell.2011.02.016
29. Kanehisa M, Goto S. *KEGG: Kyoto Encyclopedia of Genes and Genomes.* Vol 28.; 2000. <http://www.genome.ad.jp/kegg/>
30. Kutmon M, Lotia S, Evelo CT, Pico AR. WikiPathways App for Cytoscape: Making biological pathways amenable to network analysis and visualization. *F1000Res.* 2014;3:152. doi:10.12688/f1000research.4254.1
31. Slenter DN, Kutmon M, Hanspers K, et al. WikiPathways: A multifaceted pathway database bridging metabolomics to other omics research. *Nucleic Acids Res.* 2018;46(D1):D661-D667. doi:10.1093/nar/gkx1064
32. Oughtred R, Stark C, Breitkreutz BJ, et al. The BioGRID interaction database: 2019 update. *Nucleic Acids Res.* 2019;47(D1):D529-D541.
33. Stark C, Breitkreutz BJ, Reguly T, Boucher L, Breitkreutz A, Tyers M. BioGRID: a general repository for interaction datasets. *Nucleic Acids Res.* 2006;34(suppl_1):D535-D539.
34. Szklarczyk D, Franceschini A, Wyder S, et al. STRING v10: protein-protein interaction networks, integrated over the tree of life. *Nucleic Acids Res.* 2015;43(D1):D447-D452.
35. Szklarczyk D, Gable AL, Lyon D, et al. STRING v11: protein-protein association networks with increased coverage, supporting functional discovery in genome-wide experimental datasets. *Nucleic Acids Res.* 2019;47(D1):D607-D613.

36. Buyan A, Kalli AC, Sansom MSP. Multiscale Simulations Suggest a Mechanism for the Association of the Dok7 PH Domain with PIP-Containing Membranes. *PLoS Comput Biol*. 2016;12(7). doi:10.1371/journal.pcbi.1005028
37. TCGA. <https://www.cancer.gov/about-nci/organization/ccg/research/structural-genomics/tcga>.
38. Hamilton WL, Ying R, Leskovec J. Inductive representation learning on large graphs. *Adv Neural Inf Process Syst*. 2017;2017-Decem(Nips):1025-1035.
39. Veličković P, Casanova A, Liò P, Cucurull G, Romero A, Bengio Y. Graph attention networks. *6th International Conference on Learning Representations, ICLR 2018 - Conference Track Proceedings*. Published online 2018:1-12.
40. Thekumparampil KK, Wang C, Oh S, Li LJ. *Attention-Based Graph Neural Network for Semi-Supervised Learning*; 2018.
41. Shi Y, Huang Z, Feng S, Zhong H, Wang W, Sun Y. *Masked Label Prediction: Unified Message Passing Model for Semi-Supervised Classification*.
42. Nelson TJ, Xu Y. Sting and p53 DNA repair pathways are compromised in Alzheimer's disease. *Sci Rep*. 2023;13(1). doi:10.1038/s41598-023-35533-6
43. Farmer KM, Ghag G, Puangmalai N, Montalbano M, Bhatt N, Kaye R. P53 aggregation, interactions with tau, and impaired DNA damage response in Alzheimer's disease. *Acta Neuropathol Commun*. 2020;8(1). doi:10.1186/s40478-020-01012-6
44. Soelter TM, Howton TC, Clark AD, Oza VH, Lasseigne BN. Altered glia-neuron communication in Alzheimer's Disease affects WNT, p53, and NFκB Signaling determined by snRNA-seq. *Cell Communication and Signaling*. 2024;22(1). doi:10.1186/s12964-024-01686-8
45. Clark JS, Kaye R, Abate G, Uberti D, Kinnon P, Piccirella S. Post-translational Modifications of the p53 Protein and the Impact in Alzheimer's Disease: A Review of the Literature. *Front Aging Neurosci*. 2022;14. doi:10.3389/fnagi.2022.835288
46. Sharma VK, Singh TG, Singh S, Garg N, Dhiman S. Apoptotic Pathways and Alzheimer's Disease: Probing Therapeutic Potential. *Neurochem Res*. 2021;46(12):3103-3122. doi:10.1007/s11064-021-03418-7

47. Erekat NS. Apoptosis and its therapeutic implications in neurodegenerative diseases. *Clinical Anatomy*. 2022;35(1):65-78. doi:10.1002/ca.23792
48. Zhang R, Song Y, Su X. Necroptosis and Alzheimer's Disease: Pathogenic Mechanisms and Therapeutic Opportunities. *Journal of Alzheimer's Disease*. 2023;94(s1):S367-S386. doi:10.3233/JAD-220809
49. Zhang R, Song Y, Su X. Necroptosis and Alzheimer's Disease: Pathogenic Mechanisms and Therapeutic Opportunities. *Journal of Alzheimer's Disease*. 2023;94(s1):S367-S386. doi:10.3233/JAD-220809
50. Richard R, Mousa S. Necroptosis in Alzheimer's disease: Potential therapeutic target. *Biomedicine and Pharmacotherapy*. 2022;152. doi:10.1016/j.biopha.2022.113203
51. Sun E, Motolani A, Campos L, Lu T. The Pivotal Role of NF- κ B in the Pathogenesis and Therapeutics of Alzheimer's Disease. *Int J Mol Sci*. 2022;23(16). doi:10.3390/ijms23168972
52. Ge M, Zhang J, Chen S, et al. Role of Calcium Homeostasis in Alzheimer's Disease. *Neuropsychiatr Dis Treat*. 2022;18:487-498. doi:10.2147/NDT.S350939
53. Huang DX, Yu X, Yu WJ, et al. Calcium Signaling Regulated by Cellular Membrane Systems and Calcium Homeostasis Perturbed in Alzheimer's Disease. *Front Cell Dev Biol*. 2022;10. doi:10.3389/fcell.2022.834962
54. Villaseca P, Cisternas P, Inestrosa NC. Menopause and development of Alzheimer's disease: Roles of neural glucose metabolism and Wnt signaling. *Front Endocrinol (Lausanne)*. 2022;13. doi:10.3389/fendo.2022.1021796
55. Valencia-Olvera AC, Maldonado Weng J, Christensen A, LaDu MJ, Pike CJ. Role of estrogen in women's Alzheimer's disease risk as modified by APOE. *J Neuroendocrinol*. 2023;35(2). doi:10.1111/jne.13209
56. Atwood CS, Meethal SV, Smith MA, Bowen RL. *The Gonadotropin Connection in Alzheimer's Disease*. Vol 26.; 2005.
57. Casadesus G, Atwood CS, Zhu X, et al. Evidence for the role of gonadotropin hormones in the development of Alzheimer disease. *Cellular and Molecular Life Sciences*. 2005;62(3):293-298. doi:10.1007/s00018-004-4384-0

58. Raffaele I, Silvestro S, Mazzon E. MicroRNAs and MAPKs: Evidence of These Molecular Interactions in Alzheimer's Disease. *Int J Mol Sci.* 2023;24(5). doi:10.3390/ijms24054736
59. Chen MJ, Ramesha S, Weinstock LD, et al. Extracellular signal-regulated kinase regulates microglial immune responses in Alzheimer's disease. *J Neurosci Res.* 2021;99(6):1704-1721. doi:10.1002/jnr.24829
60. Rusek M, Smith J, El-Khatib K, Aikins K, Czuczwar SJ, Pluta R. The Role of the JAK/STAT Signaling Pathway in the Pathogenesis of Alzheimer's Disease: New Potential Treatment Target. *Int J Mol Sci.* 2023;24(1). doi:10.3390/ijms24010864
61. Kumar M, Bansal N. Implications of Phosphoinositide 3-Kinase-Akt (PI3K-Akt) Pathway in the Pathogenesis of Alzheimer's Disease. *Mol Neurobiol.* 2022;59(1):354-385. doi:10.1007/s12035-021-02611-7
62. Hugon J, Paquet C. The pkr/p38/riple1 signaling pathway as a therapeutic target in alzheimer's disease. *Int J Mol Sci.* 2021;22(6):1-12. doi:10.3390/ijms22063136
63. Jayaraman A, Htike TT, James R, Picon C, Reynolds R. TNF-mediated neuroinflammation is linked to neuronal necroptosis in Alzheimer's disease hippocampus. *Acta Neuropathol Commun.* 2021;9(1). doi:10.1186/s40478-021-01264-w
64. Uddin MdS, Kabir MdT, Jalouli M, et al. Neuroinflammatory Signaling in the Pathogenesis of Alzheimer's Disease. *Curr Neuropharmacol.* 2021;20(1):126-146. doi:10.2174/1570159x19666210826130210
65. Plantone D, Pardini M, Righi D, Manco C, Colombo BM, De Stefano N. The Role of TNF- α in Alzheimer's Disease: A Narrative Review. *Cells.* 2024;13(1). doi:10.3390/cells13010054
66. Liu Y, Meng Y, Zhou C, Yan J, Guo C, Dong W. Activation of the IL-17/TRAF6/NF- κ B pathway is implicated in A β -induced neurotoxicity. *BMC Neurosci.* 2023;24(1). doi:10.1186/s12868-023-00782-8
67. Yan XZ, Lai L, Ao Q, Tian XH, Zhang YH. Interleukin-17A in Alzheimer's Disease: Recent Advances and Controversies. *Curr Neuropharmacol.* 2021;20(2):372-383. doi:10.2174/1570159x19666210823110004

68. Hao W, Luo Q, Tomic I, et al. Modulation of Alzheimer's disease brain pathology in mice by gut bacterial depletion: the role of IL-17a. *Gut Microbes*. 2024;16(1). doi:10.1080/19490976.2024.2363014
69. Xu X, Wu X, Yue G, et al. The role of Nod-like receptor protein 3 inflammasome activated by ion channels in multiple diseases. *Mol Cell Biochem*. 2023;478(6):1397-1410. doi:10.1007/s11010-022-04602-1
70. Wu L, Xian X, Xu G, et al. Toll-Like Receptor 4: A Promising Therapeutic Target for Alzheimer's Disease. *Mediators Inflamm*. 2022;2022. doi:10.1155/2022/7924199
71. D'Angiolini S, Trubiani O, Mazzon E. Role of toll-like receptor signaling pathway in a rat model of spinal cord injury: a transcriptomic analysis. *Italian Journal of Anatomy and Embryology*. 2023;127(2):65-68. doi:10.36253/ijae-14689
72. Chen JR. *Characterization of the Transcriptome and TCR of Brain and Cerebrospinal Fluid Infiltrated CD8 + T Cells in an Alzheimer's Disease Mouse Model*. http://journals.aai.org/jimmunol/article-pdf/210/1_Supplement/63.21/1632118/63_21.pdf
73. Chen X, Firulyova M, Manis M, et al. Microglia-mediated T cell Infiltration Drives Neurodegeneration in Tauopathy. *Alzheimer's & Dementia*. 2023;19(S13). doi:10.1002/alz.070849
74. Wang X, Liu GJ, Gao Q, Li N, Wang R tao. C-type lectin-like receptor 2 and zonulin are associated with mild cognitive impairment and Alzheimer's disease. *Acta Neurol Scand*. 2020;141(3):250-255. doi:10.1111/ane.13196
75. Li M, Zhang R, Li J, Li J. The Role of C-Type Lectin Receptor Signaling in the Intestinal Microbiota-Inflammation-Cancer Axis. *Front Immunol*. 2022;13. doi:10.3389/fimmu.2022.894445
76. Nakamura K, Ohya W, Funakoshi H, et al. Possible role of scavenger receptor SRCL in the clearance of amyloid- β in Alzheimer's disease. *J Neurosci Res*. 2006;84(4):874-890. doi:10.1002/jnr.20992
77. Grant-Peters M, Fairbrother-Browne A, Hicks A, et al. Network nature of ligand-receptor interactions underlies disease comorbidity in the brain. doi:10.1101/2024.06.15.599140

78. Lau SF, Fu AKY, Ip NY. Receptor–ligand interaction controls microglial chemotaxis and amelioration of Alzheimer’s disease pathology. *J Neurochem*. 2023;166(6):891-903. doi:10.1111/jnc.15933
79. Wojcieszak J, Kuczyńska K, Zawilska JB. Role of Chemokines in the Development and Progression of Alzheimer’s Disease. *Journal of Molecular Neuroscience*. 2022;72(9):1929-1951. doi:10.1007/s12031-022-02047-1
80. Lombardero L, Llorente-Ovejero A, Manuel I, Rodríguez-Puertas R. Neurotransmitter receptors in Alzheimer’s disease: From glutamatergic to cholinergic receptors. In: *Genetics, Neurology, Behavior, and Diet in Dementia: The Neuroscience of Dementia, Volume 2*. Elsevier; 2020:441-456. doi:10.1016/B978-0-12-815868-5.00028-1
81. Jankowska A, Wesolowska A, Pawlowski M, Chlon-Rzepa G. Multi-Target-Directed Ligands Affecting Serotonergic Neurotransmission for Alzheimer’s Disease Therapy: Advances in Chemical and Biological Research. *Curr Med Chem*. 2017;25(17):2045-2067. doi:10.2174/0929867324666170529122802
82. Wang W, Sun T. Impact of TRPV1 on Pathogenesis and Therapy of Neurodegenerative Diseases. *Molecules*. 2024;29(1). doi:10.3390/molecules29010181
83. Lu J, Zhou W, Dou F, Wang C, Yu Z. TRPV1 sustains microglial metabolic reprogramming in Alzheimer’s disease. *EMBO Rep*. 2021;22(6). doi:10.15252/embr.202052013
84. Lee KI, Lee H Te, Lin HC, et al. Role of transient receptor potential ankyrin 1 channels in Alzheimer’s disease. *J Neuroinflammation*. 2016;13(1). doi:10.1186/s12974-016-0557-z
85. Lambris JD. *TRPC Channels and Alzheimer’s Disease*. <http://www.springer.com/series/5584>
86. Su CH, Yang WT. Association of Pulmonary Tuberculosis With Risk of Alzheimer’s: A Population-Based Cohort Study. *Respir Care*. 2018;63(Suppl 10):3017468. http://rc.rcjournal.com/content/63/Suppl_10/3017468.abstract
87. Yaghoubi A, Ghazvini kiarash, Isaac Hashemy S. *Tuberculosis for Alzheimer’s: Risk Factor, Treatment or Prevention*. Vol 7.; 2020. <http://rcm.mums.ac.ir>
88. McQuaid S, Allen I V, McMahon J, Kirk J. Association of measles virus with neurofibrillary tangles in subacute sclerosing panencephalitis: a combined in

- situ hybridization and immunocytochemical investigation. *Neuropathol Appl Neurobiol.* 1994;20(2):103-110. doi:<https://doi.org/10.1111/j.1365-2990.1994.tb01168.x>
89. Griffin DE, Lin WH, Pan CH. Measles virus, immune control, and persistence. *FEMS Microbiol Rev.* 2012;36(3):649-662. doi:10.1111/j.1574-6976.2012.00330.x
90. Nho K, Kueider-Paisley A, Ahmad S, et al. Association of Altered Liver Enzymes With Alzheimer Disease Diagnosis, Cognition, Neuroimaging Measures, and Cerebrospinal Fluid Biomarkers. *JAMA Netw Open.* 2019;2(7). doi:10.1001/jamanetworkopen.2019.7978
91. Ji M, Xie XX, Liu DQ, et al. Hepatitis B core VLP-based mis-ordered tau vaccine elicits strong immune response and alleviates cognitive deficits and neuropathology progression in Tau.P301S mouse model of Alzheimer's disease and frontotemporal dementia. *Alzheimers Res Ther.* 2018;10(1):55. doi:10.1186/s13195-018-0378-7
92. Gutierrez FRS, Guedes PMM, Gazzinelli RT, Silva JS. The role of parasite persistence in pathogenesis of Chagas heart disease. *Parasite Immunol.* 2009;31(11):673-685. doi:10.1111/j.1365-3024.2009.01108.x
93. Govindarajulu M, Ramesh S, Beasley M, et al. Role of cGAS–Sting Signaling in Alzheimer's Disease. *Int J Mol Sci.* 2023;24(9). doi:10.3390/ijms24098151
94. Mukherjee S, Huang H, Weiss LM, Costa S, Scharfstein J, Tanowitz HB. *ROLE OF VASOACTIVE MEDIATORS IN THE PATHOGENESIS OF CHAGAS' DISEASE.* Vol 8.; 2003.

Appendix

Section A

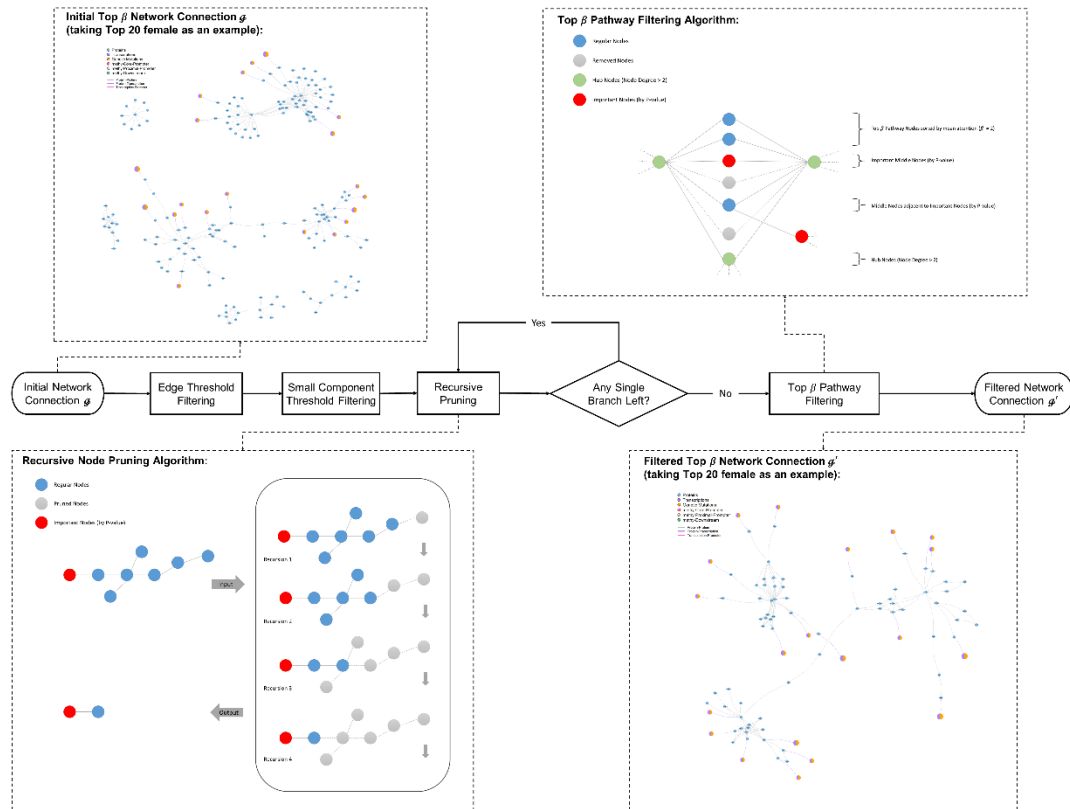


Figure S1. Diagram of the pruning procedures for core signaling networks visualization.

This pruning elucidates the systematic process of filtering and pruning network connections, essential for refining the network to its most significant components. The process begins with edge threshold filtering and small component threshold filtering. Edge threshold filtering eliminates edges that do not meet a specified significance level, thereby reducing the overall number of connections in the network. Small component threshold filtering removes smaller, less significant components from the network, focusing on the more substantial and potentially meaningful parts. Once the initial filtering is completed, a recursive node pruning algorithm is applied. This algorithm iteratively removes nodes that are deemed insignificant based on specific criteria, such as low connectivity or minimal contribution to the network's overall structure. The purpose of this pruning is to simplify the network by eliminating nodes that do not add

substantial value to the analysis, ensuring that only the most relevant nodes are retained.

After pruning, the algorithm checks whether any single branches remain within the network. A single branch is defined as a linear path with no bifurcations, which might not be as informative in the context of complex network structures. If a single branch is detected, pathway filtering is performed. Pathway filtering ensures that the remaining connections form biologically relevant pathways, thereby enhancing the network's interpretability and utility for further analysis. The final result is a filtered network connection that retains the most significant elements, providing a clearer and more focused representation of the network's structure. The diagram also includes examples of the initial and filtered network connections, illustrating the transformation that occurs through each stage of the process. Detailed steps of the recursive node pruning and pathway filtering algorithms are provided, enhancing the understanding of the methodology employed.

This meticulous approach to filtering and pruning ensures that the resulting network is not only simpler but also more biologically meaningful. By focusing on the most significant connections and pathways, researchers can achieve more accurate and insightful analyses, ultimately contributing to a deeper understanding of the underlying biological processes.